



## **Dose point kernels in liquid water: An intra-comparison between GEANT4-DNA and a variety of Monte Carlo codes.**

Christophe Champion, Sébastien Incerti, Yann Perrot, Rachel Delorme, Marie-Claude Bordage, Manuel Bardiès, Barbara Mascialino, Ngoc-Hoang Tran, Vladimir Ivanchenko, Mario Bernal, et al.

### **► To cite this version:**

Christophe Champion, Sébastien Incerti, Yann Perrot, Rachel Delorme, Marie-Claude Bordage, et al.. Dose point kernels in liquid water: An intra-comparison between GEANT4-DNA and a variety of Monte Carlo codes.. Appl Radiat Isot, 2013, epub ahead of print. <10.1016/j.apradiso.2013.01.037>. <hal-00858479>

**HAL Id: hal-00858479**

**<https://hal.archives-ouvertes.fr/hal-00858479>**

Submitted on 6 Sep 2013

**HAL** is a multi-disciplinary open access archive for the deposit and dissemination of scientific research documents, whether they are published or not. The documents may come from teaching and research institutions in France or abroad, or from public or private research centers.

L'archive ouverte pluridisciplinaire **HAL**, est destinée au dépôt et à la diffusion de documents scientifiques de niveau recherche, publiés ou non, émanant des établissements d'enseignement et de recherche français ou étrangers, des laboratoires publics ou privés.

1 **Dose Point Kernels in liquid water:**

2 **an intra-comparison between GEANT4-DNA and a variety of Monte Carlo codes**

3 C. Champion<sup>a</sup>, S. Incerti<sup>a</sup>, Y. Perrot<sup>b</sup>, R. Delorme<sup>c</sup>, M.C. Bordage<sup>d</sup>, M. Bardiès<sup>e</sup>,

4 B. Mascialino<sup>f</sup>, H.N. Tran<sup>a</sup>, V. Ivanchenko<sup>g</sup>, M. Bernal<sup>h</sup>, Z. Francis<sup>i</sup>, J.-E. Groetz<sup>j</sup>, M.

5 Fromm<sup>j</sup>, L. Campos<sup>k</sup>

6 <sup>a</sup>Université Bordeaux 1, CNRS/IN2P3, CENBG, Gradignan, France.

7 <sup>b</sup>Laboratoire de Physique Corpusculaire, Université Blaise Pascal, CNRS/IN2P3, Aubière,  
8 France.

9 <sup>c</sup>CEA, LIST, Laboratoire Modélisation, Simulation et Systèmes, Gif-sur-Yvette, France.

10 <sup>d</sup>Laboratoire Plasmas et Conversion d'énergie, Université Paul Sabatier, Toulouse, France.

11 <sup>e</sup>CRCT, UMR 1037 INSERM, Université Paul Sabatier, Toulouse, France.

12 <sup>f</sup>Department of medical radiation physics, Stockholm University, Stockholm, Sweden.

13 <sup>g</sup>Ecoanalytica, 119899 Moscow, Russia.

14 <sup>h</sup>Instituto de Física Gleb Wataghin, Universidade Estadual de Campinas, SP, Brazil.

15 <sup>i</sup>Université Saint Joseph, Science Faculty, Department of Physics, Beirut, Lebanon.

16 <sup>j</sup>Université de Franche-Comté, Laboratoire Chrono-Environnement, UMR CNRS 6249,  
17 Besançon, France.

18 <sup>k</sup>Departamento de Física, Universidade Federal de Sergipe, São Cristóvão, Brazil

19  
20 **Abstract**

21 Modelling the radio-induced effects in biological medium requires accurate physics models to  
22 describe in detail the main physical interactions induced by all the charged particles present in  
23 the irradiated medium (secondary as well as primary ones). These interactions include  
24 inelastic events like ionization and excitation processes as well as elastic scattering, the latter  
25 being the most important process in the low-energy regime. To check the accuracy of the

26 theoretical models recently implemented into the Geant4 toolkit for modelling the electron  
27 slowing-down in liquid water, the simulation of electron Dose Point Kernels remains the  
28 preferential test. In this work, normalized radial profiles of deposited energy at a distance  
29 from emissions point sources are then computed in liquid water by using the very low energy  
30 “Geant4-DNA” physics processes available in the Geant4 toolkit. We here report an extensive  
31 comparison with profiles obtained by a large selection of existing and well-documented  
32 Monte-Carlo codes, namely, EGSnrc, PENELOPE, CPA100, FLUKA and MCNPX.

33

34 **Keywords:** Dose Point Kernel; Geant4-DNA; Monte Carlo codes; liquid water.

35

36

37 **PACS:** 87.53.Bn; 02.70.Ss; 87.50.-a; 87.53.-j

38

39

40 **Corresponding author**

41 Christophe Champion

42 Université Bordeaux 1, CNRS/IN2P3, Centre d’Etudes Nucléaires de Bordeaux Gradignan,

43 CENBG, Chemin du Solarium, BP120, 33175 Gradignan, France

44 Tel: +33-5-57-12-08-89; fax: +33-5-57-12-08-01

45 E-mail address: [champion@cenbg.in2p3.fr](mailto:champion@cenbg.in2p3.fr)

46

## 47 **1. Introduction**

48 Energy deposition functions from point isotropic sources - commonly denoted dose point  
49 kernel (DPK) functions - are of prime interest in many fields like dosimetry in particular for  
50 medical applications. To better understand the radiobiological effects resulting from the use  
51 of electron-emitting radiopharmaceuticals, it is necessary to have an appropriate knowledge of  
52 the cellular distribution of the radiopharmaceutical and then to model the microscopic  
53 distribution of energy deposited in irradiated matter [1]. Absorbed doses to targeted cancer  
54 cells play an important role in evaluating the relative merits of different radionuclides and  
55 pharmaceuticals. In this context, information on the bio-distribution at the tissue, cellular and  
56 sub-cellular levels can be obtained by autoradiography [2], micro-autoradiography [3], or  
57 alternative techniques such as secondary ion mass spectrometry [4]. Converting these data to  
58 absorbed dose distribution requires the use of analytic methods based on point-dose kernels or  
59 methods based on radiation transport calculations [5-7]. Indeed, Monte Carlo code event-by-  
60 event simulations can be particularly suitable [7-11]. The latter consist in describing, step-by-  
61 step, interaction after interaction, the history of each ionizing particle created during the  
62 irradiation of the biological matter. In this kind of numerical code, each projectile-target  
63 interaction is described either thanks to theoretical (differential as well as total) cross sections  
64 or by semi-empirical ones giving access to a more or less complete description of the  
65 kinematics before and after the collision.

66 In fact, there are in the literature a large number of Monte Carlo electron track-structure  
67 codes in water, which have been developed independently to investigate the microscopic  
68 features of ionizing radiation, the ensuing chemical pathways and the molecular nature of the  
69 damages in bio-molecular targets (see [11] and references therein). The aim of the present  
70 study is to compare dose point kernels - for particular electron energies - calculated by using  
71 different Monte Carlo codes, namely, EGSnrc [12], PENELOPE [13], CPA100 [14], FLUKA

72 [15], MCNPX [16] and GEANT4-DNA [17]. To do that, the energy deposited by the emitted  
73 electrons as well as all the secondary particles produced along the primary trajectories are  
74 scored in spherical shells placed around an isotropic source for distances ranging from 0 to  
75 1.2 times the continuous slowing-down approximation range hereafter denoted  $R_{CSDA}$  and  
76 provided by the different codes here studied.

77

## 78 **2. Methods**

79 The Monte Carlo numerical simulations used in the present study are well-documented and  
80 nowadays extensively used by many groups. Only a brief description is then hereafter  
81 reported and for more details we refer the interested reader to the corresponding literature  
82 whose examples are cited as references.

### 83 *2.1 The GEANT4-DNA code*

84 The Geant4-DNA code is fully included in the general purpose Geant4 Monte Carlo  
85 simulation toolkit. It simulates track structures of electrons, hydrogen and helium atoms of  
86 different charge states ( $H^0$ ,  $H^+$ ) and ( $He^0$ ,  $He^+$ ,  $He^{2+}$ ) respectively, as well as  $C^{6+}$ ,  $N^{7+}$ ,  $O^{8+}$  and  
87  $Fe^{26+}$  ions, in liquid water. The physical processes include ionization (for all particles),  
88 electronic excitation (for electrons, protons, hydrogen atoms and  $\alpha$ -particles including their  
89 different charge states), charge exchange (for hydrogen and helium atoms with the above-  
90 mentioned charge states), and, for electrons, elastic scattering, vibrational excitation and  
91 dissociative attachment. Electron interactions cover the 7.4eV - 1MeV energy range, whereas  
92 proton and hydrogen interactions are simulated from 100eV to 100MeV while helium ions of  
93 different charged states are followed from 1keV up to 400MeV. These processes are further  
94 described in [17].

### 95 *2.2 The EGSnrc code*

96 EGSnrc is a general-purpose package for the Monte Carlo simulation of the photons and the  
97 electrons transport from a few keV up to 100GeV. EGSnrc uses a condensed history approach  
98 based on the formalism developed by Kawrakow and Bielajew to sample angular distributions  
99 from the any-angle form of the screened Rutherford cross section [18]. The Möller inelastic  
100 cross-sections are used for the generation of secondary electrons. For this study, the  
101 simulations were based on the user-code EDKnrc developed by Mainegra *et al.* [19]. We  
102 applied the PRESTA II electron-step algorithm and the EXACT boundary crossing algorithm  
103 to switch to single scattering when a particle comes closer to a boundary. The “skin depth”  
104 parameter was set to 3: it represents the number of elastic mean free paths to the next  
105 boundary at which the simulation switches into single scattering mode. We set the cut-off  
106 parameter ECUT to 1 keV in order to track primaries and secondaries until they leave the  
107 geometry or their energy falls below 1 keV. We produced a PEGS4 data set describing cross  
108 sections and stopping powers adapted for this low cut-off value.

### 109 *2.3 The PENELOPE code*

110 PENELOPE (2006 version) is a general-purpose Monte Carlo code for the coupled simulation  
111 of electron and photon transport. The cross sections database used in PENELOPE covers a  
112 wide range of elements ( $Z = 1-99$ ) and various materials useful for medical applications in the  
113 energy range of 50 eV - 1 GeV. This code has the flexibility to generate electron and positron  
114 histories on the basis of a mixed procedure, which combines detailed simulation of hard  
115 events with the continuous slowing down approximation for soft interactions. The level of  
116 detail of electron transport processes is controlled in PENELOPE by specifying values for  
117 several parameters,  $C_1$ ,  $C_2$ ,  $W_{CC}$  and  $W_{CR}$ . The  $C_1$  and  $C_2$  parameters are associated to the  
118 condensation of electron and positron elastic scattering processes.  $W_{CC}$  and  $W_{CR}$ , respectively,  
119 represent the cut-off energy losses for hard inelastic collisions and for hard Bremsstrahlung  
120 emission. A detailed description of the algorithms used in PENELOPE can be found in its

121 manual [20]. These simulations were done with detailed event-by-event transport setting  
122  $C_1 = C_2 = 0$ ,  $W_{CC} = W_{CR} = 50$  eV and using 50 eV as the lower absorption energy allowed in  
123 this code.

#### 124 *2.4 The CPA100 code*

125 CPA100 is an event by event Monte Carlo track structure code, developed in Toulouse  
126 (France), for understanding fundamental aspects of radiation track interaction [14]. It  
127 simulates complete electron/photon transport in liquid water for energy range from 10 to  
128 200 keV. It generates all the electronic and photonic cascades occurring after a particle  
129 passage in the volume of interest (Auger electron, X-Rays, atomic reorganization). It is also  
130 able to describe the various stages of the particle transport not only the early physical stage,  
131 but also the physico-chemical and the chemical ones, during the very early passage of  
132 particles in matter say up to one microsecond. Primary physical and chemical damages not  
133 only in liquid water but also in complex DNA targets and its higher order structures can be  
134 calculated to estimate the radio-induced damage to the DNA molecular scale (DSB, SSB,  
135 base lesion).

#### 136 *2.5 The FLUKA code*

137 FLUKA is a multi-purpose Monte Carlo particle transport code that considers all particle  
138 interactions including electromagnetic interactions, nuclear interactions of the primary or  
139 incident particles and the generated secondary particles, energy loss fluctuations and Coulomb  
140 scattering [15]. The version 2011.2.15 with the default configuration 'PRECISION' was used,  
141 with an energy cut-off lowered at 1 keV for electrons and 0.1 keV for photons. To reach a  
142 good accuracy, the single scattering model through the 'MULSOPT' option was activated,  
143 because the Moliere multiple scattering model could be unreliable with thin shells, disturbing  
144 the propagation of electrons between the boundaries [21].

#### 145 *2.6. The MCNPX code*



146 MCNPX is a general-purpose Monte Carlo code for modelling the interaction of radiation  
147 with matter [16]. MCNPX stands for MCNP eXtended and transports electrons, photons,  
148 neutrons and several particle types, like nearly all energies. It utilizes the latest nuclear cross  
149 section libraries and covers various materials useful for medical applications. The tallies have  
150 extensive statistical analysis and the convergence is enabled by a wide variety of variance  
151 reduction methods. For this work, the version 2.7.0 was used with the F8\* energy deposition  
152 tally in coupled electron-photon mode. The photon and electron cut-off energies were set  
153 above 1 keV. A specific consideration was focused on electron transport conditions, through  
154 the ITS option and the ESTEP parameter, due to the very narrow shells. The ITS energy  
155 indexing algorithm was used to have a better definition of the energy group and their  
156 boundaries [22] and the ESTEP parameter was increased in order to divide the major electron  
157 energy step into smaller sub-steps [23]: ESTEP = 10 for 100 keV and ESTEP = 100 for 10, 30  
158 and 50 keV.

159

### 160 **3. Results and discussion**

161 To obtain the dose point kernel (DPK) around an isotropic point source, the geometry  
162 here used consists in a spherical water phantom divided into 120 spherical shells of thickness  
163  $R_{CSDA}/100$ , where  $R_{CSDA}$  stands for the continuous-slowing-down-approximation range whose  
164 values calculated by the different codes here studied are reported in Table 1. Note that for the  
165 EGSnrc, the CPA100, the FLUKA and the MCNPX codes, the corresponding values are taken  
166 from the NIST web database ESTAR [24], what generates stopping powers and ranges for  
167 electrons which are the same as those tabulated in ICRU Report 37 [25]. Besides, let us  
168 remind that the present GEANT4-DNA version transports electrons down to an energy  
169 threshold of 7.4 eV contrary to the other codes studied which use higher energy cut-off, what  
170 undoubtedly affects the  $R_{CSDA}$  values.

171 Finally, the GEANT4-DNA DPK distributions have been compared to those obtained  
 172 with the other Monte Carlo codes by using Kolmogorov-Smirnov statistical tests. Thus, we  
 173 found that the GEANT4-DNA simulations are statistically compatible with EGSnrc and  
 174 PENELOPE simulations ( $p$ -value  $> 0.05$ ) with a maximum distance ( $D$ ) between distribution  
 175 functions less than 0.2. On the contrary, much smaller  $p$ -values ( $< 0.05$ ) and larger  $D$   
 176 distances were obtained when comparing GEANT4-DNA simulations with the MCNPX and  
 177 CPA100 simulations.

178 The DPK distributions also obtained by the different numerical codes are reported in  
 179 Figure 1 for four particular electron energies, namely, 10 keV, 30 keV, 50 keV and 100 keV.  
 180 These quantities are defined as the fraction of the emitted energy absorbed (per unit mass) at a  
 181 certain distance from the point source and are usually reported by means of scaled  
 182 distributions defined as  $F(r/R_{CSDA}) = \frac{\delta E(r)/E_0}{\delta r/R_{CSDA}}$  where  $r$  is the distance from the point source,  
 183  $\delta E(r)$  stands for the energy absorbed in the spherical shell sited at a distance  $r$  from the point  
 184  $r/R_{CSDA}$  source,  $E_0$  being the initial kinetic energy of the electron and  $\delta r$  the shell thickness  
 185 (here  $R_{CSDA}/100$ ). The obtained distributions will be hereafter reported as a function of  $r/R_{CSDA}$   
 186 and refer to scoring of the deposited energy at the mid-radius of the shell.

187 In Figure 1, we observe that the shape of the dose point kernels generated by the  
 188 different codes is very similar. However, we note that the CPA100 code exhibits a peak closer  
 189 to the source in comparison to the other codes ( $r/R_{CSDA} \cong 0.53$  vs 0.58), the amplitudes being  
 190 all of the same order of magnitude - from 1.45 to 1.55 - except for the MCNPX which largely  
 191 overestimates the other results. When the incident electron energy increases, these  
 192 observations are confirmed with in particular an improvement of the agreement between the  
 193 CPA100 and the other simulations. Thus, from Fig.1b) to Fig.1d) all the curves tend to  
 194 converge except again the MCNPX simulation which provides higher DPKs (of about 20%).

195 Besides, for the four energetic cases here reported, the GEANT4-DNA DPK  
196 distributions have been compared to those obtained with the other Monte Carlo codes by  
197 using Kolmogorov-Smirnov statistical tests. Thus, we found that the GEANT4-DNA  
198 simulations are statistically compatible with EGSnrc, PENELOPE and FLUKA simulations  
199 ( $p$ -value  $> 0.05$ ) with a maximum distance ( $D$ ) between distribution functions less than 0.3.  
200 On the contrary, much smaller  $p$ -values ( $< 0.05$ ) and larger  $D$  distances were obtained when  
201 comparing GEANT4-DNA simulations with the MCNPX (for the four incident energy  
202 values) and CPA100 (for 30 keV and 50 keV) simulations.

#### 203 204 **4. Conclusions**

205 Normalized radial profiles of deposited energy - commonly referred to as dose point kernels -  
206 have been here reported by using the very low energy “Geant4-DNA” physics processes  
207 available in the Geant4 toolkit. In comparison with profiles obtained by a large selection of  
208 existing and well-documented Monte-Carlo codes, namely, EGSnrc, PENELOPE, CPA100,  
209 FLUKA and MCNPX, we have here emphasized evident discrepancies undoubtedly related to  
210 the physics models implemented into the different codes. In this context, the Geant4-DNA  
211 code has been shown to provide accurate dose point kernels for incident electron energies  
212 ranging from 10 keV to 100 keV.

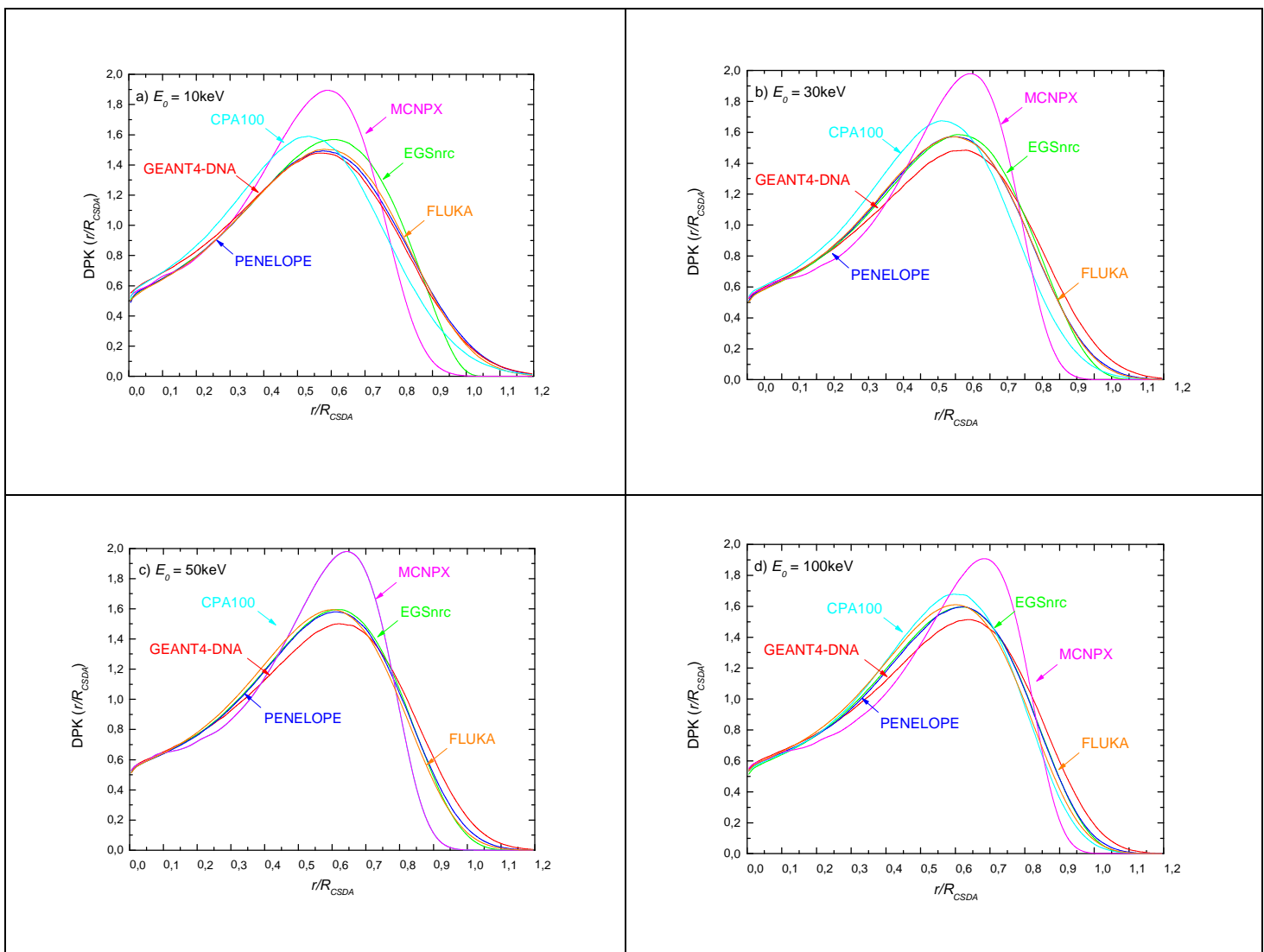
#### 213 214 **Acknowledgements**

215 The Geant4-DNA project received funding partly from the French Agence Nationale de la  
216 Recherche under contract number ANR-09-BLAN-0135-01 and from the European Space  
217 Agency under contract number AO6041- 22712/09/NL/AT. This work has been developed as  
218 part of the activities planned in the project PICS 5921 (THEOS) of the Centre National de la  
219 Recherche Scientifique.

220 **Figure 1:**

221 (Color online) Comparison between the scaled dose point kernel distributions obtained by the  
222 different numerical track-structure codes studied in the present work: GEANT4-DNA (red),  
223 EGSnrc (green), PENELOPE (blue), CPA100 (cyan), MCNPX (magenta) and FLUKA  
224 (orange). Panel a)  $E_0 = 10$  keV. Panel b)  $E_0 = 30$  keV. Panel c)  $E_0 = 50$  keV.  
225 Panel d)  $E_0 = 100$  keV.

226



227

228 **Table 1:**

229 Comparison between the continuous-slowing-down-approximation range  $R_{CSDA}$  ( $\mu\text{m}$ ) obtained  
230 by the different numerical track-structure codes studied in the present work.

$E_0$	$R_{CSDA}$ (GEANT4-DNA)	$R_{CSDA}$ (PENELOPE)	$R_{CSDA}^*$ (EGSnrc, CPA100, KLUKA, MCNPX)
<b>10 keV</b>	2.76	2.52	2.52
<b>30 keV</b>	18.16	17.57	17.56
<b>50 keV</b>	44.07	43.21	43.20
<b>100 keV</b>	144.12	143.06	143.10

231 *\*Note that the EGSnrc, CPA100, FLUKA and MCNPX values have been taken from the NIST*  
232 *web database ESTAR [24] contrary to the other data here reported.*

233

234 **References**

- 235 [1] A.I. Kassis, Radiobiologic principles in radionuclide therapy, *J. Nucl. Med.* **46** (2005)  
236 4S12S.
- 237 [2] E.D. Yorke, L.E. Williams, A.J. Demidecki, D.B. Heidorn, P.L. Roberson, B.W. Wessels,  
238 Multicellular dosimetry for beta-emitting radionuclides: autoradiography, thermoluminescent  
239 dosimetry and three-dimensional dose calculations, *Med. Phys.* **20** (1993) 543-550.
- 240 [3] M.R. Puncher, P.J. Blower, Radionuclide targeting and dosimetry at the microscopic level:  
241 the role of microautoradiography, *Eur. J. Nucl. Med.* **21** (1994) 1347-1365.
- 242 [4] F. Chehade, C. de Labriolle-Vaylet, N. Moins, M.F. Moreau, J. Papon, P. Labarre,  
243 P. Galle, A. Veyre, E. Hindié, Secondary ion mass spectrometry as a tool for investigating  
244 radiopharmaceutical distribution at the cellular level: the example of I-BZA and <sup>14</sup>C-I-BZA,  
245 *J. Nucl. Med.* **46** (2005) 1701-1706.
- 246 [5] W.E. Bolch, L.G. Bouchet, J.S. Robertson, B.W. Wessels, J. A. Siegel, R.W. Howell,  
247 A.K. Erdi, B. Aydogan, S. Costes, E.E. Watson, A.B. Brill, N.D. Charkes, D.R. Fisher, M.T.  
248 Hays, S.R. Thomas, MIRD Pamphlet No. 17: the dosimetry of nonuniform activity  
249 distributions-radionuclide S values at the voxel level. Medical Internal Radiation Dose  
250 Committee, *J. Nucl. Med.* **40** (1999) 11S-36S.
- 251 [6] L. Strigari, E. Menghi, M. d'Andrea, M. Benassi, Monte Carlo dose voxel kernel  
252 calculations of beta-emitting and Auger-emitting radionuclides for internal dosimetry: a  
253 comparison between EGSnrcMP and EGS4, *Med. Phys.* **33** (2006) 3383-3389.
- 254 [7] W.B. Li, W. Friedland, E. Pomplun, P. Jacob, H. Paretzke, M. Lassmann, C.H.R. Reiners,  
255 Track structures and dose distributions from decays of <sup>131</sup>I and <sup>125</sup>I in and around water  
256 spheres simulating micrometastases of differentiated thyroid cancer, *Radiat. Res.* **156** (2001)  
257 419-429.

258 [8] C. Champion, Theoretical cross sections for electron collisions in water: structure of  
259 electron tracks, *Phys. Med. Biol.* **48** (2003) 2147-2168.

260 [9] C. Champion, A. L'hoir, M.F. Politis, P.D. Fainstein, R.D. Rivarola, A. Chetioui, A  
261 Monte Carlo code for the simulation of heavy-ion tracks in water, *Radiat. Res.* **163** (2005)  
262 222-231.

263 [10] C. Champion, C. Le Loirec, Positron follow-up in liquid water. I. A new Monte Carlo  
264 track-structure code, *Phys. Med. Biol.* **5** (2006) 1707-1723.

265 [11] S. Uehara, H. Nikjoo, D.T. Goodhead, Comparison and assessment of electron cross  
266 sections for Monte Carlo track structure codes, *Radiat. Res.* **152** (1999) 202-13.

267 [12] I. Kawrakow, Accurate condensed history Monte Carlo simulation of electron transport :  
268 I. EGSnrc, the new EGS4 version, *Med. Phys.* **27** 485-98 (2000).

269 [13] S. Salvat, J.M. Fernandez-Varea, J. Sempau, PENELOPE-2006, A Code System for  
270 Monte Carlo Simulation of Electron and Photon Transport, OECD ISBN 92-64-02301-1  
271 (2006).

272 [14] M. Terrissol and A. Baudre, A simulation of space and time evolution of radiolytic  
273 species induced by electrons in water, *Radiat. Prot. Dosim.* **31** (1990) 175-177.

274 [15] FLUKA: A Multi-Particle Transport Code. Geneva: CERN European organization for  
275 nuclear research; 2005.

276 [16] MCNPX User's Manual, Version 2.5.0, Laurie Waters, ed., LA-CP-05-0369 (2005).  
277 <http://mcnpx.lanl.gov/documents.html>.

278 [17] S. Incerti, A. Ivanchenko, M. Karamitros, A. Mantero, P. Moretto, H.N. Tran, B.  
279 Mascialino, C. Champion, V.N. Ivanchenko, M.A. Bernal, Z. Francis, C. Villagrasa, G.  
280 Baldacchino, P. Guèye, R. Capra, P. Nieminen, C. Zacharatou, Comparison of GEANT4 very  
281 low energy cross section models with experimental data in water, *Med. Phys.* **37** (2010) 4692-  
282 4708.

283 [18] I. Kawrakow and A.F. Bielajew, On the representation of electron multiple elastic-  
284 scattering distributions for Monte Carlo calculations, Nucl. Instrum. Methods Phys. Res. B  
285 **134** (1998) 325-35.

286 [19] E. Mainegra-Hing, D.W.O. Rogers, I. Kawrakow, Calculation of photon energy  
287 deposition kernels and electron dose point kernels in water, Med. Phys. **32** (2005) 685-699.

288 [20] F. Salvat, J. Sempau, and J.M. Fernandez-Varea, Tech. Rep., Universitat de Barcelona,  
289 2006.

290 [21] F. Botta, A. Mairani, G. Battistoni, M. Cremonesi, A. Di Dia, A. Fassò, A. Ferrari, M.  
291 Ferrari, G. Paganelli, G. Pedroli, M. Valente, Calculation of electron and isotopes dose point  
292 kernels with FLUKA Monte Carlo code for dosimetry in nuclear medicine therapy, Med.  
293 Phys. **38** (2011) 3944-3954.

294 [22] D.R. Schaart, J.T.M Jansen, J. Zoetelief, P. De Leege, A comparison of MCNP4C  
295 electron transport with ITS 3.0 and experiment at energies between 100 keV and 20 MeV:  
296 Influence of voxel size, substeps and energy indexing algorithm, Phys. Med. Biol. **47** (2002),  
297 1459-1484.

298 [23] H. Koivunoro, T. Siiskonen, P. Kotiluoto, I. Auterinen, E. Hippeläinen, S. Savolainen,  
299 Accuracy of the electron transport in MCNP5 and its suitability for ionization chamber  
300 response simulations: A comparison with the EGSNRC and PENELOPE codes, Med. Phys.  
301 **39** (2012) 1335-1343.

302 [24] ESTAR, National Institute of Standards and Technology, « Stopping powers and Range  
303 table for electrons », <http://physics.nist.gov/PhysRefData/Star/Text/ESTAR.html>.

304 [25] ICRU, « Stopping powers for electrons and positrons », ICRU Report 37, ICRU,  
305 Washington, DC, 1984.